TROAP regulates prostate cancer progression via the WNT3/survivin signalling pathways

JIANQING YE[1*], CHUANMIN CHU[1*], MING CHEN[2*], ZHAN SHI[3*], SISHUN GAN[1], FAJUN QU[1],
XIUWU PAN[1], QIWEI YANG[1], YIJUN TIAN[1], LEI WANG[1], WEI YANG[1] and XINGANG CUI[1]

[1]Department of Urology, Third Affiliated Hospital, The Second Military Medical University, Shanghai 201805;
[2]Department of Urology, Affiliated Changzheng Hospital, The Second Military Medical University, Shanghai 200003;
[3]Department of Urology, Taizhou First People's Hospital, Taizhou, Zhejiang 318020, P.R. China

Abstract. Prostate cancer (PCa) is one of the most commonly diagnosed malignancies, and 90% of advanced prostate cancer patients relapse after therapy. Trophinin associated protein (TROAP) is essential for centrosome integrity and proper bipolar organisation of spindle assembly during mitosis and plays an essential role in proliferation. We found that *TROAP* expression correlates with patient survival and speculated that it may be involved in PCa progression. The Oncomine database tool (http://www.oncomine.org) was used to analyse TROAP mRNA expression from microarray data, and patient survival analysis for target genes was performed using the PROGgeneV2 Database (http://watson.compbio.iupui.edu). Gene interference with lentivirus was used to silence TROAP expression in PCa cells and knockdown efficiency was detected by qRT-PCR and western blot analysis. Cell viability, colony formation, cell cycle and apoptosis were then assessed to determine the function of TROAP in PCa cells. Markers of cell cycle and apoptosis were tested by western blotting. The correlation between WNT3 or survivin expression and TROAP transcripts in prostate cancer tissues was analysed using GEPIA (http://gepia.cancer-pku.cn) and validated by western blotting. The *in vivo* role of TROAP was investigated using xenografts. This protein was overexpressed in PCa, and exhibited relatively higher expression in PCa cell lines, DU145 and 22Rv1. Importantly, analysing human cancer databases available from PROGgeneV2 showed that higher expression of TROAP is associated with shorter overall survival in prostate cancer patients. TROAP knockdown inhibited cell proliferation and led to cell cycle arrest at S phase in 22Rv1

Correspondence to: Dr Xingang Cui, Department of Urology, Third Affiliated Hospital, The Second Military Medical University, 700 North Moyu Road, Shanghai 201805, P.R. China
E-mail: cuixingang@smmu.edu.cn

*Contributed equally

and DU145 cells. Cell cycle arrest resulted in apoptosis in both cell lines via the cyclin A2-cyclin B1-caspase pathway. WNT3 and survivin expression levels were found to correlate with TROAP in PCa, and *in vivo* xenograft assays revealed that silencing of TROAP inhibited PCa tumour growth. Therefore, TROAP might represent a novel predictive marker to guide therapeutic intervention.

Introduction

Prostate cancer (PCa) is one of the most commonly diagnosed malignancies and the third most common lethal cancer in men (1). Over 160,000 new cases of prostate cancer were estimated to have been diagnosed in 2017 in the US, which accounts for 19% of all cancer cases (2). Consequently, it is vitally important and necessary to study the associated detailed mechanisms of this disease.

TROAP, also named tastin and first cloned in 1995, is a cytoplasmic protein that is necessary for the function of trophinin as a cell adhesion molecule (3,4). The associated adhesion molecule complex consists of bystin, trophinin and TROAP, and bystin has been shown to be present in human PCa (5). In addition to its function as a component of the adhesion complex during embryo implantation, TROAP has also been reported to be required for spindle assembly during mitosis (6,7). It is also essential for centrosome integrity and proper bipolar organisation of spindle assembly during mitosis, playing an essential role in cell proliferation. Levels of this protein peak during the G2/M phase and abruptly decline after division. However, its biological function in prostate cancer and cancer in general is still unclear. We found that *TROAP* expression correlates with patient survival and deduced that TROAP plays an important role in prostate cancer progression.

In this study, we first examined the TROAP expression profile using several online datasets of prostate cancer; in addition, patient survival analysis with respect to the target gene was performed using PROGgeneV2 Database. Next, the regulatory effect of TROAP on cellular survival and apoptosis was demonstrated by performing cell proliferation and flow cytometric assays. Western blot analysis was used to determine the expression of apoptosis and cell cycle-related biomarkers. Correlations between WNT3 or survivin expression and

TROAP transcripts in prostate cancer tissues were also analysed. Finally, the regulation of TROAP in PCa cell progression was established *in vivo*. Collectively, our data suggest that TROAP could be an important target for PCa diagnosis and treatment.

Materials and methods

Database analysis. To examine TROAP mRNA expression using microarray data, the Oncomine database tool (www. oncomine.org) was used. Briefly, the *TROAP* gene was queried in the database and the results were filtered by selecting prostate cancer studies that reported *TROAP* expression data (Reporter ID: 204649_at for Varambally Prostate, Arredouani Prostate, Wallace Prostate and A_23_P150935 for Grasso Prostate). Both probes were targeted to nucleotide sequence of TROAP. P-values for each group were calculated using The Student's t-test. Standardised normalisation techniques and statistical calculations are provided by the Oncomine website. Additionally, ProggeneV2 prognostic Database (http://watson. compbio.iupui.edu/chirayu) was used to collect information about patient survival data with regards to TROAP expression in prostate cancer (8).

Cell lines and culture conditions. Human prostate cell lines, LNCaP, WPMY-1, DU145, 22Rv1, PC-3 and C4-2 (all have been confirmed that they are not misidentified or contaminated by checking established cell lines with the list of known misidentified cell lines available from the International Cell Line Authentication Committee http://iclac.org/databases/cross-contaminations) were purchased from the Cell Bank of the Chinese Academy of Science (Shanghai, China). LNCaP and WPMY-1 cells were cultured in DMEM (Hyclone Laboratories; GE Healthcare Life Sciences, Logan, UT, USA; SH30022.01B) with 10% fetal bovine serum (FBS). C4-2 and 22RV1 cells were cultured in RPMI-1640 medium (Hyclone Laboratories; GE Healthcare Life Sciences, SH30809.01B) containing 10% FBS (Biowest, Riverside, MO, USA; S1810). DU145 and PC-3 cells were cultured in Ham's/F-12 (Gibco; Thermo Fisher Scientific, Inc., Waltham, MA, USA; 11765054) with 10% FBS and 1% non-essential amino acids (NEAA, Hyclone Laboratories; GE Healthcare Life Sciences; SH30238.01). The culture medium was supplemented with 100 U/ml penicillin and 100 mg/ml streptomycin to avoid bacterial contamination. All cells were cultured in humidified air at 37°C with 5% CO_2.

Total RNA isolation and quantitative real-time (qRT)-PCR analysis. Total RNA was prepared from several human prostate cancer cell lines (WPMY-1, LNCap, 22Rv1, DU145, PC3 and C4-2) using TRIzol reagent (Invitrogen; Thermo Fisher Scientific, Inc.) following the manufacturer's protocol. Then, 1 μg of total RNA was reverse transcribed in a final volume of 20 μl using random primers and M-MLV Reverse Transcriptase (Promega, Madison, WI, USA; M170A) and standard conditions. The reverse transcription reaction was performed using the following conditions: 37°C for 30 min; 85°C for 5 sec and a hold at 4°C.

After reverse transcription, the qRT-PCR was performed using the SYBR Green Master Mix Kit (Takara Biotechnology,

Co., Ltd., Dalian, China) and a BioRad CFX96 sequence detection system, according to the manufacturer's instructions. The relative levels of TROAP were determined by qRT-PCR using gene specific primers, and expression was normalised to the internal control β-actin. The primer sequences used are as follows: forward, 5'-GTGGACATCCGCAAAGAC-3' and reverse, 5'-AAAGGGTGTAACGCAACTA-3' for β-actin, and forward, 5'-GGTCAGGAGAAAAGCGGAGGAAG-3' (sense) and reverse, 5'-AGGCGTGCGTTTCTGAGAGC-3' for TROAP. The qRT-PCR was conducted under the following conditions: 95°C for 60 sec, 40 cycles of 95°C for 5 sec and 60°C for 20 sec. Each sample was run at least three times. The relative expression level of TROAP was computed using the comparative cycle threshold (CT) method $2^{-\Delta\Delta Cq}$ (9).

Lentivirus infection of prostate cancer cells. The shRNA sequence targeting TROAP was synthesised and ligated into pGreenPuro™ shRNA Cloning and Expression Lentivector (#s SI505A-1; SBI System Biosciences, LLC, Palo Alto, CA, USA), which contains green fluorescent protein (GFP) tag. The shRNA sequence targeting human TROAP was: 5'-AGAACCAAGATCCAAGGAGATCTCGAGATCTCCTTGGATCTTGGTTCT-3'. The non-targeting shCon sequence (control shRNA) used was 5'-TTCTCCGAACGTGTCACGTCTCGAGACGTGACACGTTCGGAGAA-3'. Lentiviral particles were then packaged in the 93T cells and harvested using ultra-centrifugation. DU145 and 22Rv1 cell lines cultured in 6-well plates were infected with lentivirus containing targeting shRNA or control shRNA. Cells were harvested after 3 days for qRT-PCR and other experiments.

Cell proliferation assays. The effect of TROAP knockdown on cell proliferation was determined using the 3-(4,5-dimethyl-2-thiazolyl)-2,5-diphenyl-2H-tetrazolium bromide (MTT) method according to the manufacturer's (Sigma-Aldrich; Merck KGaA) instructions. Briefly, DU145 and 22Rv1 cells infected with shTROAP and shCon, separately, were seeded in 96-well plates (3,000/well) and incubated for 5 days. At day 1 to day 5 after seeding, MTT plus acidic isopropanol solution was added to every well and samples were incubated at 37°C for 1 h. The absorbance values were measured at 595 nm using a Biotek Epoch Microplate Spectrophotometer (BioTek Instruments, Inc., Winooski, VT, USA). Each group comprised five replicates.

Colony formation assays. For colony formation assays, DU145 and 22Rv1 cells were seeded in 6-well plates at 500 cells/well and cultured in medium containing 10% FBS, changing the medium every 3 days. After 14 days, the colonies were washed with PBS, fixed with 4% paraformaldehyde, and stained with 0.1% freshly-prepared crystal violet solution (Beyotime Unstitute of Biotechnology, Haimen, China). Visible colonies containing 50 or more cells were observed and manually counted using an inverted light microscope (Olympus CKX41; Olympus Corp., Tokyo, Japan). Triplicate wells were measured for each treatment group.

Flow cytometric analysis. For flow cytometric analysis, infected cells were collected 6 days after inoculation by trypsinisation. Cells for cell cycle analysis were stained using
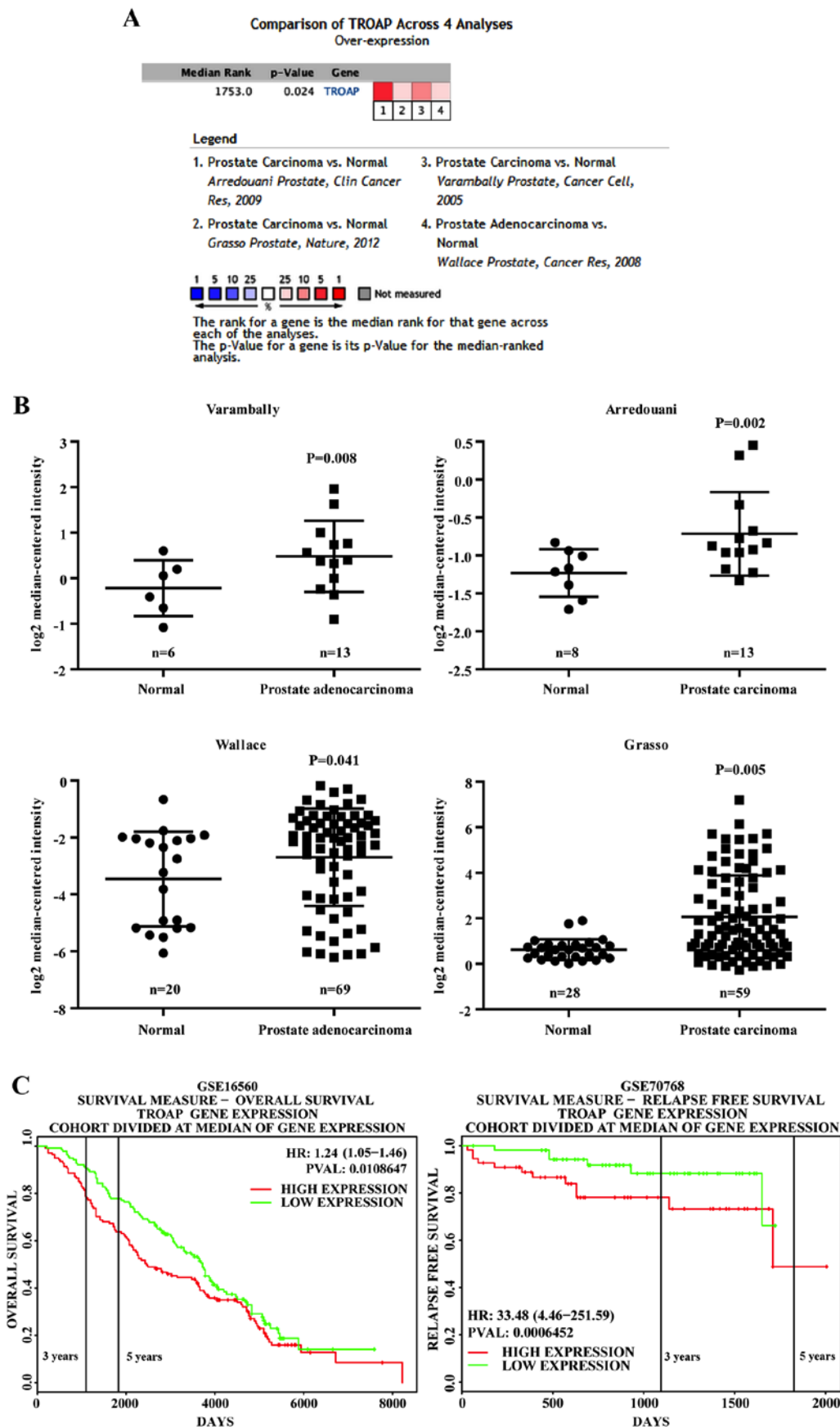
Figure 1. TROAP is overexpressed in prostate cancer and higher expression is associated with shorter overall survival. (A) Oncomine analysis of the prostate cancer datasets showed that four datasets reported overexpression of TROAP in cancer as compared to expression in normal tissue. (B) Representation of individual datasets reporting TROAP expression from the Oncomine website and analysed using an unpaired Student's t-test. (C) Higher expression of TROAP was associated with shorter overall survival (left) and relapse-free survival (right) of prostate cancer patients. Survival data were retrieved and analysed from PROGgeneV2 (http://watson.compbio.iupui.edu/chirayu/proggene/database/? url=proggene). Patients were grouped based on TROAP expression levels, specifically, higher or lower than the median level.
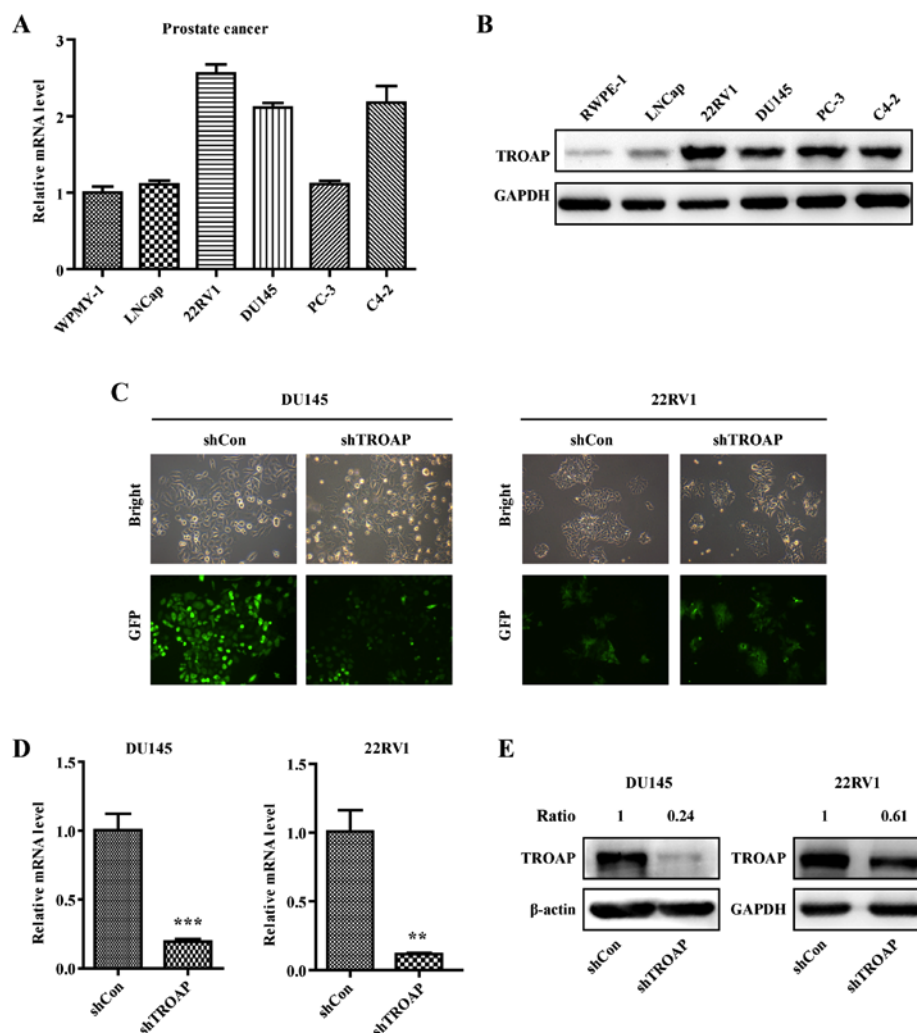
Figure 2. TROAP expression and efficiency of lentivirus-mediated TROAP shRNA silencing in prostate cancer cell lines. (A) The mRNA expression level of TROAP in prostate cancer cells (LNCap, 22RV1, DU145, PC-3 and C4-2) and normal cancer cells (WPMY-1). (B) The protein levels of TROAP in prostate cancer and normal cells. (C) Representative images of prostate cancer cell lines infected with shCon/shTROAP lentivirus are shown. (D) Analyses of TROAP mRNA expression in DU145 and 22Rv1 cells quantified by qRT-PCR. **P<0.01 and ***P<0.001 vs. shCon. (E) Western blot analyses of TROAP protein expression in DU145 and 22Rv1 cells. Data are presented as means ± SD of three independent experiments.

propidium iodide (PI) with the Cycle TEST PLUS DNA Reagent kit (BD Biosciences, Franklin Lakes, NJ, USA; NC9941088) according to the manufacturer's protocol, and then subjected to FACScan. The percentage of the cells in the G0/G1, S, and G2/M phases were computed and compared. For apoptosis analysis, double staining was performed using the FITC Annexin V Apoptosis Detection kit (Nanjing KeyGen Biotech, Co., Ltd., Nanjing, China), according to the manufacturer's instructions, and then the stained cells were analysed using FACScan (BD Biosciences). The percentage of early apoptotic and apoptotic cells were compared to that in the control groups for each experiment.

Western blot assay. Cells were lysed using RIPA buffer containing 100 mM Tris-HCl (pH 6.8), 10 mM EDTA, 4% SDS, and 10% glycine supplemented with PMSF (Roche, Basel, Switzerland). Total protein was quantified using the Coomassie brilliant blue method at 560 nm. The supernatant (10 μg of protein) was denatured and separated on 12% SDS polyacrylamide gel electrophoresis (SDS-PAGE), and then transferred to 0.22-μm polyvinylidene difluoride (PVDF)

membranes (EMD Millipore, Bedford, MA, USA) and incubated with specific antibodies as follows: anti-GAPDH (dilution 1:500,000; cat. no. 10494-1-AP), anti-TROAP (dilution 1:1,000; cat. no. 13634-1-AP), anti-PSA (dilution 1:1,000; cat. no. 10679-1-AP), anti-cleaved caspase 3 (dilution 1:1,000; cat. no. 25546-1-AP), anti-caspase 9 (dilution 1:1,000; cat. no. 10380-1-AP), anti-cyclin A2 (dilution 1:1,000; cat. no. 18202-1-AP), anti-WNT3 (dilution 1:500; cat. no. 17983-1-AP), anti-survivin (dilution 1:1,000; cat. no. 10508-1-AP) and anti-CNNB1 (dilution 1:1,000; cat. no. 51067-2-AP) from Proteintech Group Inc., (Rosemont, IL, USA); anti-Bcl-2 (dilution 1:1,000; cat. no. 2876) and PARP (dilution 1:1,000; cat. no. 9542) from Cell Signaling Technology, Inc. (Danvers, MA, USA); anti-cyclin B1 (dilution 1:2,000; cat. no. 21540) from SAB (Nanjing, China). Bands were visualised using enhanced chemiluminescence (ECL-PLUS/Kit, Amersham Pharmacia Biotech, Tokyo, Japan) reagents.

Pairwise correlation analysis. WNT3 and survivin were previously reported to be relevant for carcinogenesis. To determine whether there is a correlation between the expression of
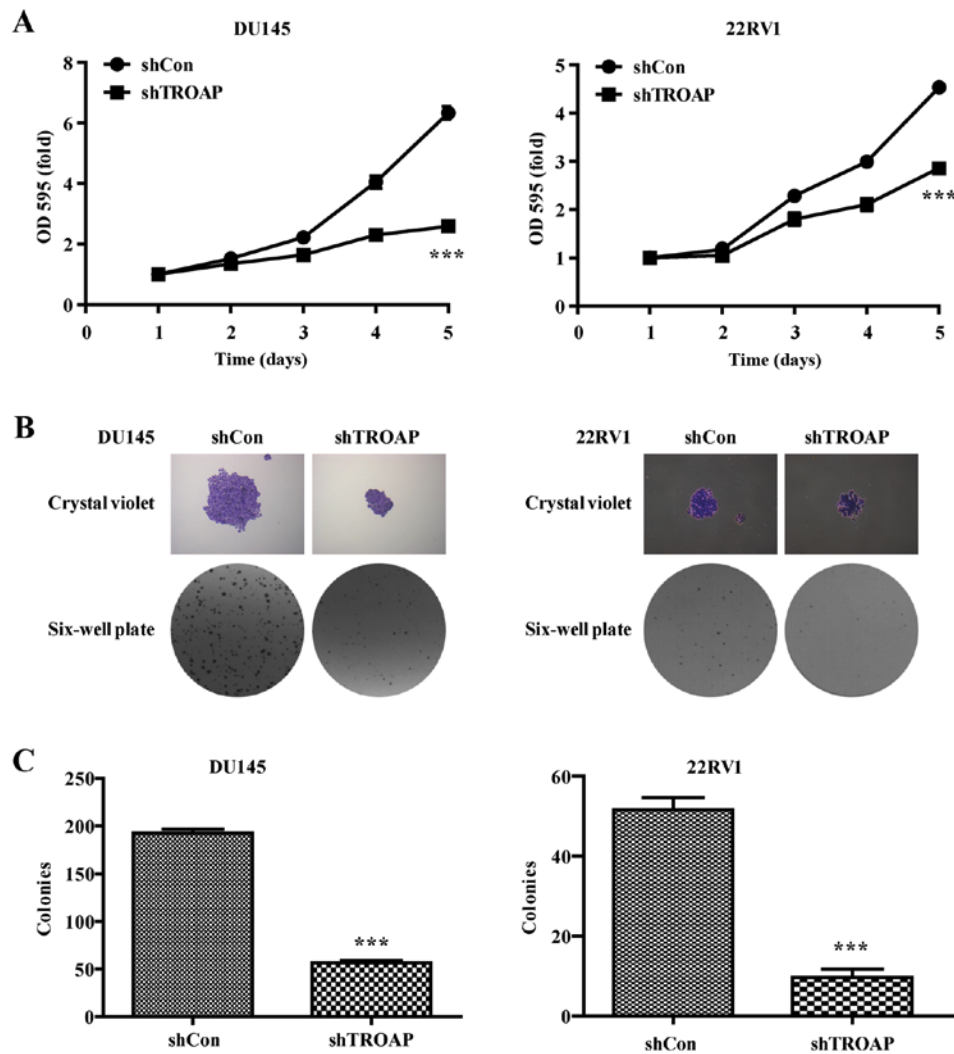
Figure 3. Effects of TROAP knockdown on the proliferation and colony formation of DU145 and 22Rv1 prostate cancer cells. (A) Cell viability was determined by MTT assays. (B) Representative images of crystal violet staining and colony size and density in DU145 and 22Rv1 cells. (C) Statistical analysis of colony numbers in shCon- and shTROAP-infected cells. Data are shown as means ± SD of three independent experiments. ***P<0.001 vs. shCon.

WNT3 or survivin and *TROAP* transcripts in PCa, pairwise gene correlation analysis was performed using the web server GEPIA (http://gepia.cancer-pku.cn/) (10). P<0.05 was defined as statistically significant. Correlation analysis results were then further validated by western blot analysis.

Xenograft tumourigenicity and gene expression assay in vivo. The prior approval of the Ethics Committee of the Third Affiliated Hospital, The Second Military Medical University was obtained for use of the animals in this study.

Twelve male athymic nude mice (nu/nu), 4 weeks old (weight, 15-20 g), were housed under pathogen-free conditions in a barrier animal facility with a 12-h light/12-h dark cycle and humidity (45-55%) at 21-24°C, and food and water were available *ad libitum*. For *in vivo* tumourigenicity experiments, DU145 cells stably infected with lentivirus or negative control were collected, resuspended in PBS, and injected subcutaneously into the right subaxillary of each male 4-week-old BALB/c nude mouse ($2x10^4$ per mouse; SLRC Laboratory Animal, Shanghai, China). The tumour volumes and weights were measured every 3 days and maximum allowable tumour size was controlled according to the IACUC guidelines

(diameter, 2.0 cm; volume 4.2 cm^3); tumour volume (V) was measured as V = length x width^2 x 0.5. Forty-five days after injection, mice were sacrificed by cervical dislocation and tumours were dissected, imaged, and weighed; the tumours were also collected and fixed for further western blot analysis. The relative amount of protein was calculated based on the integrated optical density reference value using ImageJ optical density gel analysis software (National Institutes of Health, Bethesda, MD, USA). GAPDH was used as the control.

Statistical analysis. Statistical analysis was performed using GraphPad Prism 5.0 software (GraphPad Software, Inc., La Jolla, CA, USA). Student's t-test was used for two-group comparisons and ANOVA with Sidak's multiple comparisons were used to test the significance of multigroup data. Data are presented as mean ± SD. A P-value <0.05 was considered to be indicative of statistical significance.

Results

TROAP is overexpressed in PCa and higher expression is associated with shorter overall survival. To achieve a profound
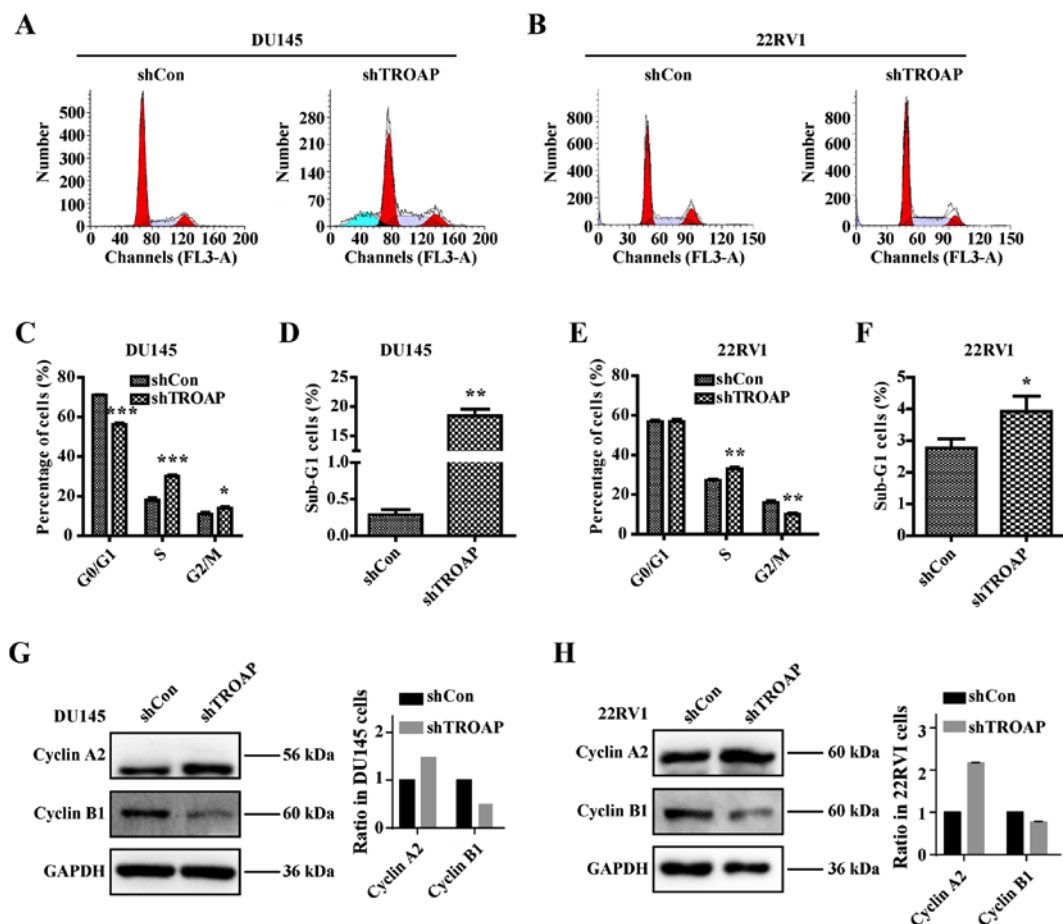
Figure 4. TROAP silencing leads to cell cycle arrest at S phase in the DU145 and 22Rv1 prostate cancer cells. (A and B) Cell cycle distribution was analysed by flow cytometry. Representative images of three independent FACS analyses are presented. (C-F) Proportions of cells in the different cell cycle phases. $^*P<0.05$, $^{**}P<0.01$ and $^{***}P<0.001$ vs. shCon. (G and H) Western blot analysis of cyclin A2 and cyclin B1 in DU145 and 22Rv1 cells with or without TROAP knockdown.

understanding of the role of TROAP in PCa, a publicly available array data source, the Oncomine database tool (www.oncomine.org), was first used to investigate the expression levels of *TROAP*. The Oncomine Cancer Microarray database contains several datasets comparing human prostate carcinoma to normal tissue. TROAP expression was commonly highly expressed in several PCa groups compared to that in adjacent normal tissue. As shown in Fig. 1A and B, four datasets [Arredouani *et al* (11), Grasso *et al* (12), Varambally *et al* (13) and Wallace *et al* (14)] showed that TROAP is significantly overexpressed in PCa as compared to levels in adjacent normal tissue, with fold changes ranging from 1.27 to 2.08 (11-14). Additionally, by exploring the PROGgeneV2 Prognostic Database, we found that PCa patients (GSE16560) (15) with TROAP levels that were higher than the median expression level had significant shorter overall survival than those with lower TROAP levels (Fig. 1C). Notably, another database (GSE70768) (16) showed that higher TROAP expression is associated with poor relapse-free survival (Fig. 1C).

TROAP expression in prostate cells and knockdown efficiency in PCa cell lines. The expression of TROAP in different PCa cell lines including WPMY-1, LNCaP, 22Rv1, DU145, PC3 and C4-2 was detected by qRT-PCR and western blotting. The results showed that the expression of TROAP is relatively high in PCa cells, especially non-metastatic

22Rv1 and metastatic DU145 cells (Fig. 2A and B), which are androgen-independent PCa cell lines. Accordingly, these two cell lines were selected for further study. DU145 and 22Rv1 cells were separately infected with the shTROAP and shCon lentiviruses. Based on the observed expression of GFP using a microscope, the infection efficiencies were adequate (Fig. 2C). Results of qRT-PCR illustrated that the mRNA levels of TROAP were significantly suppressed in DU145 and 22Rv1 cells (Fig. 2D). Accordingly, the protein levels of TROAP were decreased obviously with shRNA targeting in DU145 and 22Rv1 cells (Fig. 2E).

Inhibition of PCa cell proliferation by shRNA-mediated TROAP knockdown. To determine the effect of different treatments on PCa cell proliferation, prostate cancer cell numbers were assessed using MTT and colony formation assays. As shown by the cell growth curve, growth of the shTROAP-treated groups was significantly slower than that of the shCon groups for DU145 and 22Rv1 cells (Fig. 3A). Furthermore, the sizes of independent colonies were much smaller in DU145 and 22RV1 cells infected with shTROAP, compared to that in cells infected with shCon (Fig. 3B). Moreover, the numbers of colonies formed in shTROAP-infected groups were significantly lower than that in shCon-infected groups (P<0.001, Fig. 3C). The data demonstrated a significant reduction in cell expansion with reduced TROAP expression.
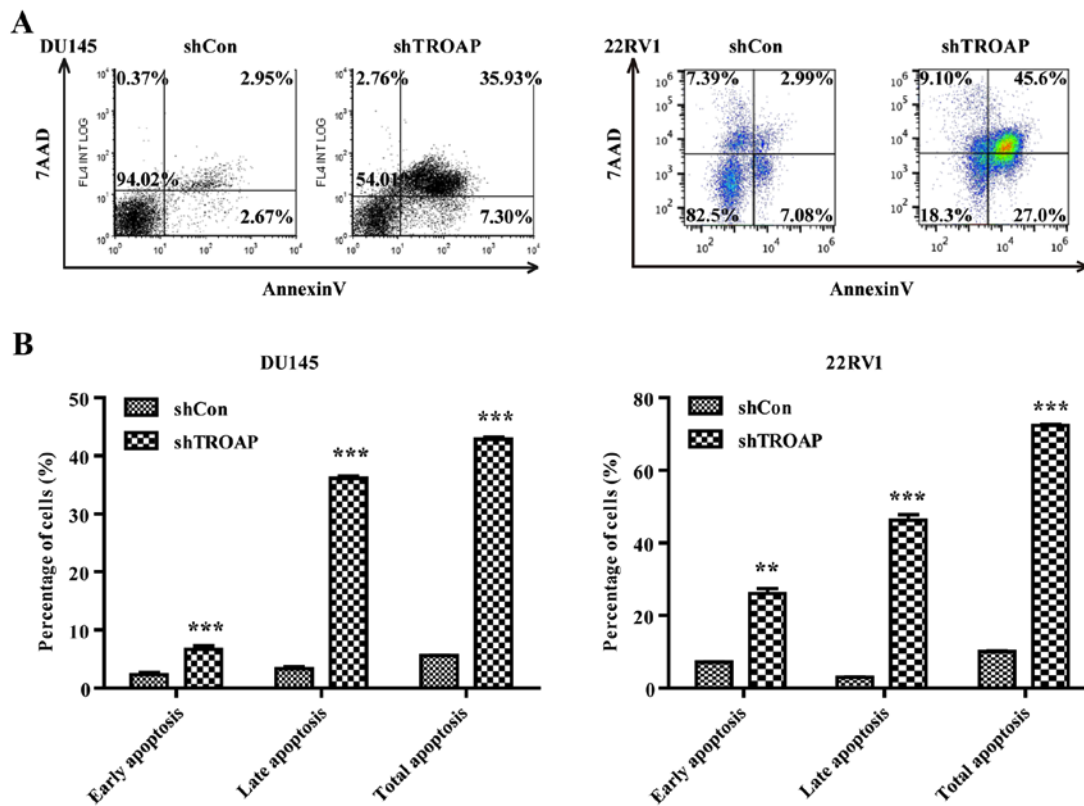
Figure 5. TROAP silencing leads to DU145 and 22Rv1 prostate cancer cell apoptosis. (A) Representative images of apoptosis in DU145 and 22Rv1 cells. (B) Cell populations with different apoptosis status were calculated. **P<0.01 and ***P<0.001 vs. shCon.
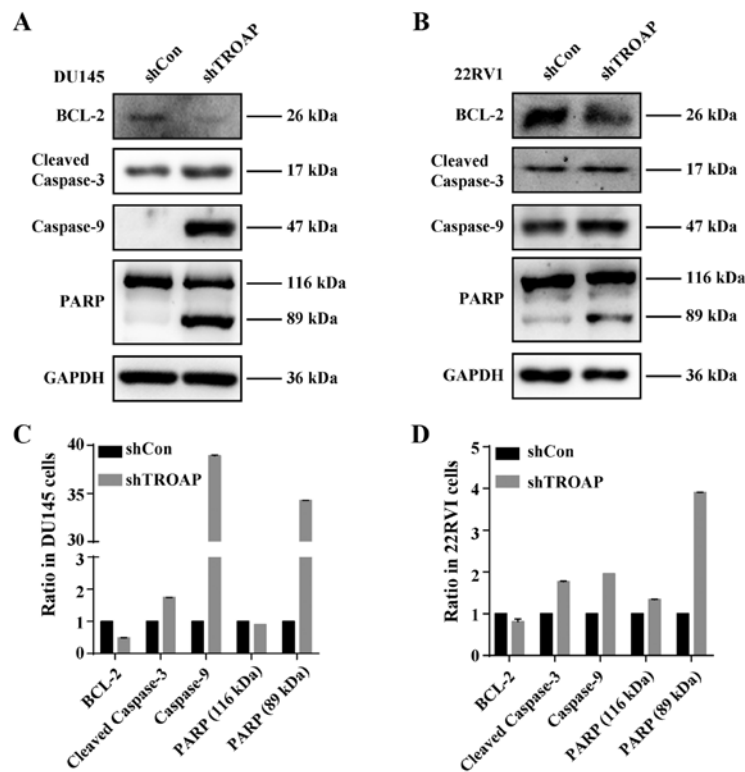

Figure 6. TROAP regulates cyclin A2/cyclinB1 and caspase-3 cascades in prostate cancer cells. (A-D) Western blot analysis of Bcl-2, caspase-9, cleaved caspase-3, and PARP (cleaved or not) in DU145 and 22Rv1 cells with TROAP ablation.

Knockdown of TROAP leads to cell cycle arrest and cell cycle modulation through cyclin A2/cyclinB1. Having

established that TROAP expression is related to PCa cell proliferation, we were next interested in whether the cell
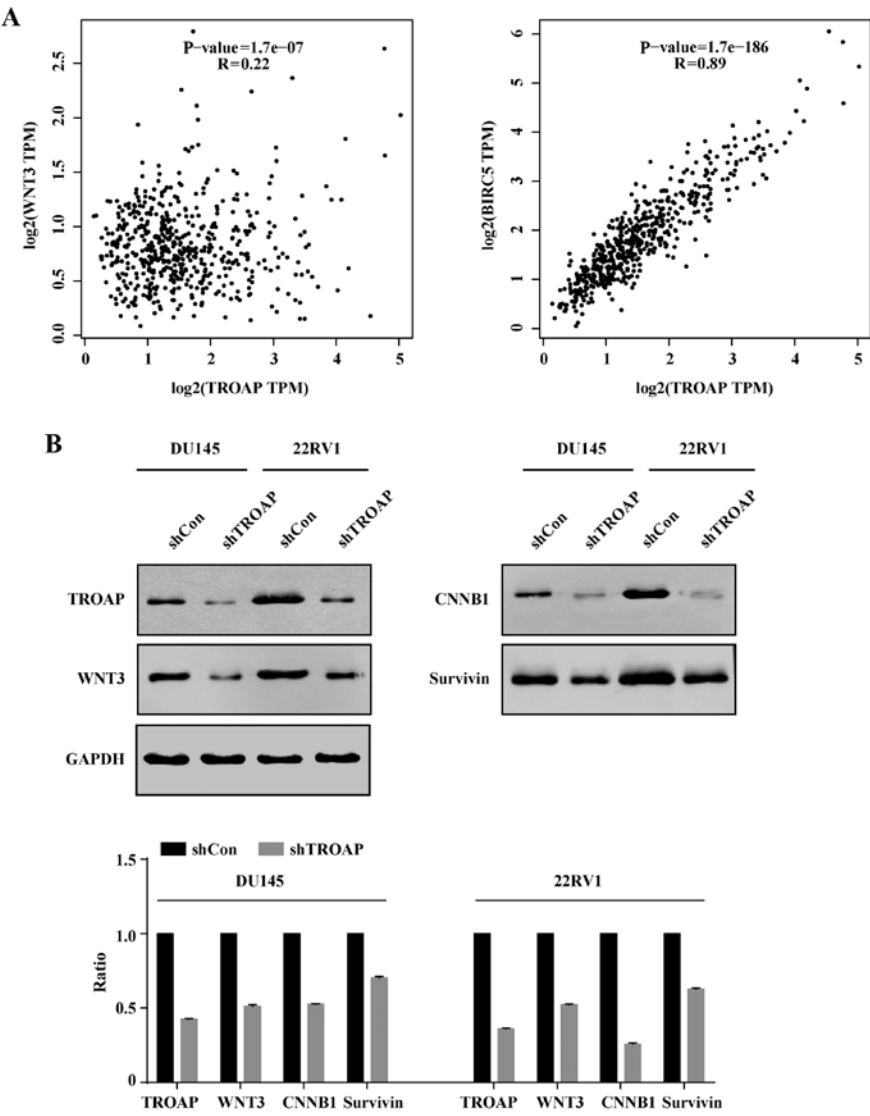
Figure 7. Expression of WNT3 and survivin is positively correlated with TROAP in prostate cancer. (A) The levels of (left) WNT3 (R=0.22, P=0.000285) and (right) survivin (BIRC5) (R=0.89, P=0.000302) were positively correlated with TROAP mRNA levels in prostate cancer based on the TCGA public dataset using GEPIA correlation analysis. (B) Western blotting further verified that WNT3 and survivin expression levels were correlated with TROAP in the DU145 and 22RV1 cell lines.

cycle is influenced by TROAP. After performing cell cycle analysis by flow cytometry, we found that inhibition of TROAP significantly decreased the number of cells in the G0/G1 phase and increased the number of cells in the S phase in the DU145 and 22Rv1 cells (Fig. 4A and B). The S phase cell percentage was increased from 18% in the shCon group to 30% in the shTROAP group in DU145 cells and from 27% in the shCon group to 33% in the shTROAP group in the 22Rv1 cells (Fig. 4C and E). TROAP knockdown further led to significant increases in the sub-G1-phase cell population in both DU145 and 22Rv1 cells (Fig. 4D and F). We then focused on the molecular mechanisms through which TROAP knockdown delays S phase to mitosis transition by analysing the expression of checkpoint proteins. Western blotting showed that downregulation of TROAP increased the expression of cyclin A2 but decreased the expression of cyclin B1, compared to that in respective controls, for the DU145 and 22Rv1 cells (Fig. 4G and H). The results thus corresponded to a cell cycle arrest at S phase.

Knockdown of TROAP promotes apoptosis in PCa cell lines through the mitochondrial apoptosis pathway. Based on the observed increases in the sub-G1-phase cell population (Fig. 4D and F), we attempted to determine whether the decrease in TROAP was associated with cancer cell apoptosis by flow cytometry. TROAP silencing significantly accelerated both DU145 and 22Rv1 cell apoptosis. Lentivirus-mediated shRNA increased both early and late apoptosis in the DU145 and 22Rv1 cells (Fig. 5A and B). The total percentage of apoptotic cells increased from 6% in the shCon group to 43% in the shTROAP group for DU145 cells, and from 10% in the shCon group to 72% in the shTROAP group for 22Rv1 cells. To investigate the underlying mechanisms of TROAP knockdown-induced apoptosis in these cells, the protein levels of Bcl-2, caspase-9, cleaved-caspase-3 and PARP in PCa cells were measured by western blot analysis after treatment with shTROAP. Western blot analysis showed that depletion of TROAP decreased the levels of Bcl-2, whereas levels of caspase-9, caspase-3 and PARP increased (Fig. 6). The results
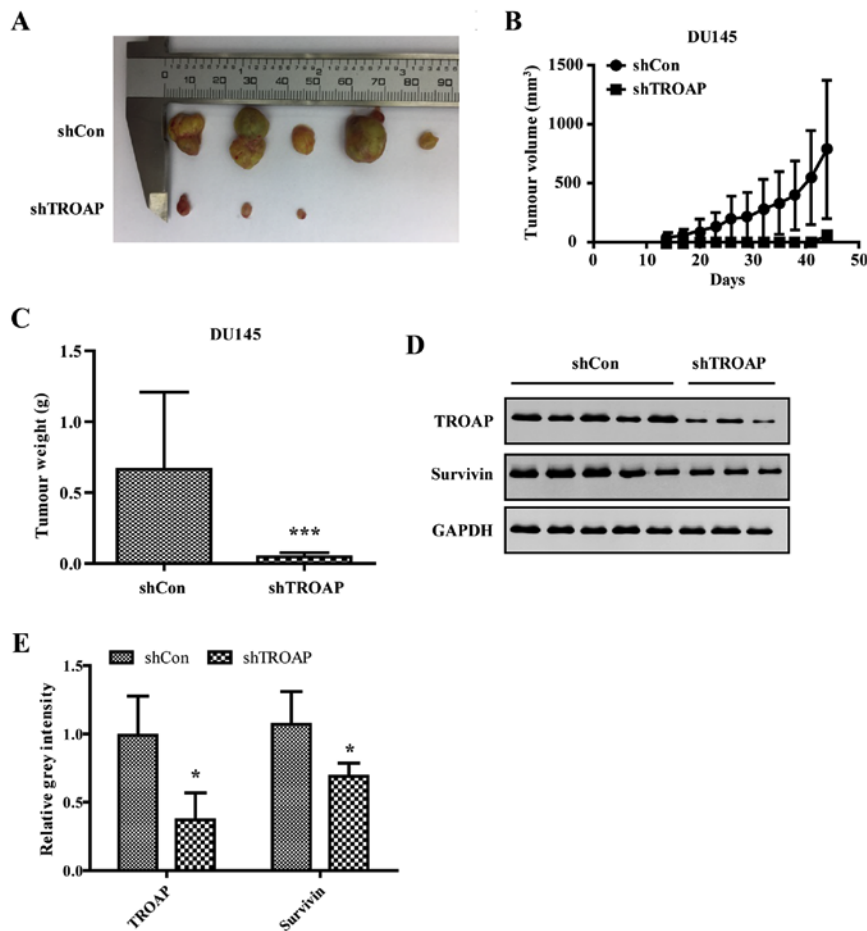
Figure 8. TROAP knockdown inhibits prostate tumour growth *in vivo*. (A) Xenograft tumours derived from shTROAP-infected DU145 cells were significantly smaller in terms of volume (B) and weight (C) when compared with these parameters in the tumours derived from the shCon-transfected cells. **P<0.001. (D) TROAP and survivin protein expression in cancer tissues was analysed by western blotting. (E) The relative protein expression of TROAP and survivin was clearly downregulated. GAPDH was used as a control, and the difference was statistically significant (*P<0.05).

demonstrated that the mitochondrial apoptosis pathway was activated by downregulation of TROAP in PCa cells.

TROAP expression correlates with WNT3 and survivin levels in PCa. Survivin is demonstrated to protect cells from caspase-induced apoptosis. Meanwhile, it was the downstream target of wnt/β-catenin. Hence, we deduced that TROAP induced apoptosis by interrupting the expression of surviving and wnt. Correlation analysis indicated that WNT3 and survivin (BIRC5) levels were positively correlated with TROAP expression (P<0.05; Fig. 7A). To further validate this analysis, we performed western blotting. Consistently, it was verified that protein levels of WNT3 and survivin decreased with TROAP knockdown (Fig. 7B).

Knockdown of TROAP inhibits PCa growth in nude mice. To investigate the effect of TROAP on PCa cell proliferation *in vivo*, a xenograft model was utilised to assess the tumorigenesis of DU145 cells after shTROAP or shCon transduction. As shown, the largest diameter of the tumours was approximately 10 mm in the shCon group. Tumours in mice injected with shTROAP-transduced cells were significantly smaller than those originating from shCon-infected cells (Fig. 8A). Both the volume and the weight of tumours derived from shTROAP DU145 cells were significantly decreased compared

to those of the shCon group (Fig. 8B and C). Thus, the results confirmed that TROAP knockdown can inhibit PCa tumour growth *in vivo*.

To further illustrate that tumour suppression by shTROAP is associated with the knockdown of TROAP and associated downregulation of survivin in PCa cells, mice from the two groups were sacrificed after the last measurement. Protein expression levels of both TROAP and survivin were detected by western blotting. As shown in Fig. 8D and E, the levels of both were efficiently decreased in tumour tissue of the shTROAP group compared to those in the shcontrol group.

Discussion

In the present study, we initially demonstrated that TROAP is upregulated in PCa tissues. Importantly, clinical data have suggested that TROAP is associated with poor overall and relapse-free survival in prostate cancer patients, underscoring the oncogenic role of this marker, particularly in relapse. We also demonstrated for the first time that TROAP protein expression is relatively high in several PCa cell lines by using qRT-PCR and western blot analysis.

Silencing of TROAP significantly inhibited the growth and colony formation ability of PCa cells through cell cycle arrest at the S phase and the induction of apoptosis.

More importantly, downregulation of TROAP dramatically decreased cyclin B1 and Bcl-2 levels and increased cyclin A2, caspase-9 protein levels and cleaved PARP.

Knockdown of TROAP caused cell cycle arrest and apoptosis through the cyclin/Cdk pathway. Cyclin A2 is a core cell cycle regulator that activates Cdk1 and Cdk2 (17). The expression of cyclin A2 and CDK2, are known to promote S phase entry in mammals (18). Cyclin B1 is a key regulator of cell cycle progression from the S phase to the G2/M phase and its downregulation therefore results in S phase arrest (19). Therefore, upregulation of cyclin A2 and downregulation of cyclin B1, induced by TROAP silencing, explains why PCa cells were arrested at the S phase. Furthermore, it was found that in the shTROAP group, the G2/M phase cell ratio was increased in DU145 cells and decreased G2/M in 22RV1 cells. This may be owing to the different metastatic abilities in DU145 and 22RV1 cells as metastasis may relate to the cell cycle (20,21). This needs further study. In addition, more cell cycle markers are required to determine the exact point at which the cell cycle is disrupted.

To further confirm that apoptosis induced by TROAP depletion is associated with the mitochondrial pathway, the levels of Bcl-2, cleaved caspase-3, caspase-9, and PARP were detected by western blotting. The results demonstrated that the mitochondrial pathway was activated by downregulation of TROAP in PCa cells. Survivin is the smallest member of the human IAPs (inhibitor of apoptosis proteins) and is the downstream target gene of the Wnt signalling pathway. WNT3, a member of the Wnt family, was reported to be associated with hepatic, lung, and colorectal carcinogenesis (22-25). It can protect cells from caspase-induced apoptosis, activated in mitosis, presumably by binding caspase-3, -7, and -9 (26). The results of the correlation analysis indicated that TROAP expression was correlated with WNT3 and survivin in PCa. Knockdown of TROAP could decrease the Wnt 3 and survivin expression, which confirms both the *in vitro* and *in vivo* experiments. Hence, we deduced that TROAP may affect proliferation through the WNT signalling pathway.

In conclusion, knockdown of TROAP decreased cell proliferation and colony formation and induced cell cycle arrest and apoptosis *in vitro*. Taken together, we concluded that TROAP functions as a regulator of PCa to control tumour growth.

In conclusion, collectively, our observations indicate that TROAP is one of the driving mechanisms of Wnt/β-catenin signalling. Our findings provide new insights into the mechanism of the progression of PCa.

Acknowledgements

Not applicable.

Availability of data and materials

The data used and/or analysed during the present study can be obtained from the corresponding author on reasonable request.

Authors' contributions

JY, CC, MC and ZS performed the vector construction experiments and drafted the manuscript. SG and FQ participated in the RT-PCR and western blot experiments. XP, QY and YT participated in the cellular function experiments. LW and WY participated in the animal experiments and were responsible for the data analysis and for the figure formation. XC participated in the research design, reviewed the literature and performed data examination. All authors read and approved the manuscript and agree to be accountable for all aspects of the research in ensuring that the accuracy or integrity of any part of the work are appropriately investigated and resolved.

Ethics approval and consent to participate

Animal experiments in this study were approved by the Ethics Committee of the Third Affiliated Hospital, The Second Military Medical University.

Patient consent for publication

Not applicable.

Competing interests

The authors state that they have no competing interests.

References

1. Siegel RL, Miller KD and Jemal A: Cancer statistics, 2016. CA Cancer J Clin 66: 7-30, 2016.
2. Hoffman RM, Meisner AL, Arap W, Barry M, Shah SK, Zeliadt SB and Wiggins CL: Trends in United States prostate cancer incidence rates by age and stage, 1995-2012. Cancer Epidemiol Biomarkers Prev 25: 259-263, 2016.
3. Fukuda MN, Sato T, Nakayama J, Klier G, Mikami M, Aoki D and Nozawa S: Trophinin and tastin, a novel cell adhesion molecule complex with potential involvement in embryo implantation. Genes Dev 9: 1199-1210, 1995.
4. Nadano D, Nakayama J, Matsuzawa S, Sato TA, Matsuda T and Fukuda MN: Human tastin, a proline-rich cytoplasmic protein, associates with the microtubular cytoskeleton. Biochem J 364: 669-677, 2002.
5. Ayala GE, Dai H, Li R, Ittmann M, Thompson TC, Rowley D and Wheeler TM: Bystin in perineural invasion of prostate cancer. Prostate 66: 266-272, 2006.
6. Yang S, Liu X, Yin Y, Fukuda MN and Zhou J: Tastin is required for bipolar spindle assembly and centrosome integrity during mitosis. FASEB J 22: 1960-1972, 2008.
7. Li CW and Chen BS: Investigating core genetic-and-epigenetic cell cycle networks for stemness and carcinogenic mechanisms, and cancer drug design using big database mining and genome-wide next-generation sequencing data. Cell Cycle 15: 2593-2607, 2016.
8. Goswami CP and Nakshatri H: PROGgeneV2: Enhancements on the existing database. BMC Cancer 14: 970, 2014.
9. Livak KJ and Schmittgen TD: Analysis of relative gene expression data using real-time quantitative PCR and the 2(-Delta Delta C(T)) Method. Methods 25: 402-408, 2001.
10. Tang Z, Li C, Kang B, Gao G, Li C and Zhang Z: GEPIA: A web server for cancer and normal gene expression profiling and interactive analyses. Nucleic Acids Res 45: W98-W102, 2017.

11. Arredouani MS, Lu B, Bhasin M, Eljanne M, Yue W, Mosquera JM, Bubley GJ, Li V, Rubin MA, Libermann TA, *et al*: Identification of the transcription factor single-minded homologue 2 as a potential biomarker and immunotherapy target in prostate cancer. Clin Cancer Res 15: 5794-5802, 2009.
12. Grasso CS, Wu YM, Robinson DR, Cao X, Dhanasekaran SM, Khan AP, Quist MJ, Jing X, Lonigro RJ, Brenner JC, *et al*: The mutational landscape of lethal castration-resistant prostate cancer. Nature 487: 239-243, 2012.
13. Varambally S, Yu J, Laxman B, Rhodes DR, Mehra R, Tomlins SA, Shah RB, Chandran U, Monzon FA, Becich MJ, *et al*: Integrative genomic and proteomic analysis of prostate cancer reveals signatures of metastatic progression. Cancer Cell 8: 393-406, 2005.
14. Wallace TA, Prueitt RL, Yi M, Howe TM, Gillespie JW, Yfantis HG, Stephens RM, Caporaso NE, Loffredo CA and Ambs S: Tumor immunobiological differences in prostate cancer between African-American and European-American men. Cancer Res 68: 927-936, 2008.
15. Sboner A, Demichelis F, Calza S, Pawitan Y, Setlur SR, Hoshida Y, Perner S, Adami HO, Fall K, Mucci LA, *et al*: Molecular sampling of prostate cancer: A dilemma for predicting disease progression. BMC Med Genomics 3: 8, 2010.
16. Ross-Adams H, Lamb AD, Dunning MJ, Halim S, Lindberg J, Massie CM, Egevad LA, Russell R, Ramos-Montoya A, Vowler SL, *et al*; CamCaP Study Group: Integration of copy number and transcriptomics provides risk stratification in prostate cancer: A discovery and validation cohort study. EBioMedicine 2: 1133-1144, 2015.
17. Hochegger H, Takeda S and Hunt T: Cyclin-dependent kinases and cell-cycle transitions: Does one fit all? Nat Rev Mol Cell Biol 9: 910-916, 2008.
18. Ding H, Han C, Guo D, Wang D, Chen CS and D'Ambrosio SM: OSU03012 activates Erk1/2 and Cdks leading to the accumulation of cells in the S-phase and apoptosis. Int J Cancer 123: 2923-2930, 2008.
19. Xu X, Zhang H, Zhang Q, Huang Y, Dong J, Liang Y, Liu HJ and Tong D: Porcine epidemic diarrhea virus N protein prolongs S-phase cell cycle, induces endoplasmic reticulum stress, and up-regulates interleukin-8 expression. Vet Microbiol 164: 212-221, 2013.
20. Basak S, Jacobs SB, Krieg AJ, Pathak N, Zeng Q, Kaldis P, Giaccia AJ and Attardi LD: The metastasis-associated gene Prl-3 is a p53 target involved in cell-cycle regulation. Mol Cell 30: 303-314, 2008.
21. Song H, Hur I, Park HJ, Nam J, Park GB, Kong KH, Hwang YM, Kim YS, Cho DH, Lee WJ, *et al*: Selenium Inhibits Metastasis of Murine Melanoma Cells through the Induction of Cell Cycle Arrest and Cell Death. Immune Netw 9: 236-242, 2009.
22. Nambotin SB, Tomimaru Y, Merle P, Wands JR and Kim M: Functional consequences of WNT3/Frizzled7-mediated signaling in non-transformed hepatic cells. Oncogenesis 1: e31, 2012.
23. Kato S, Hayakawa Y, Sakurai H, Saiki I and Yokoyama S: Mesenchymal-transitioned cancer cells instigate the invasion of epithelial cancer cells through secretion of WNT3 and WNT5B. Cancer Sci 105: 281-289, 2014.
24. Voloshanenko O, Erdmann G, Dubash TD, Augustin I, Metzig M, Moffa G, Hundsrucker C, Kerr G, Sandmann T, Anchang B, *et al*: Wnt secretion is required to maintain high levels of Wnt activity in colon cancer cells. Nat Commun 4: 2610, 2013.
25. Wang HS, Nie X, Wu RB, Yuan HW, Ma YH, Liu XL, Zhang JY, Deng XL, Na Q, Jin HY, *et al*: Downregulation of human Wnt3 in gastric cancer suppresses cell proliferation and induces apoptosis. OncoTargets Ther 9: 3849-3860, 2016.
26. Li Z, Pei XH, Yan J, Yan F, Cappell KM, Whitehurst AW and Xiong Y: CUL9 mediates the functions of the 3M complex and ubiquitylates survivin to maintain genome integrity. Mol Cell 54: 805-819, 2014.